



Fabrication, characterization and electrochemical properties of porous coral-structured Si/C composite anode for lithium ion battery

Fen-ling TANG^{1,2}, Jian-fei LEI³, Zhao-yang CUI¹, Jian OUYANG¹, Gang LIU¹, Ling-zhi ZHAO^{1,4}

1. Key Laboratory of Nanophotonic Functional Materials and Devices of Guangdong Province, Institute of Opto-Electronic Materials and Technology, South China Normal University, Guangzhou 510631, China;
2. Guangdong Food and Drug Vocational-Technical School, Guangzhou 510663, China;
3. School of Physics and Engineering, Henan University of Science and Technology, Luoyang 471023, China;
4. Guangdong Engineering Technology Research Center of Low Carbon and Advanced Energy Materials, Guangzhou 510631, China

Received 20 January 2015; accepted 26 June 2015

Abstract: A porous coral-structured Si/C composite as an anode material was fabricated by coating Si nanoparticles with a carbon layer from polyvinyl alcohol (PVA), erosion of hydrofluoric (HF) acid, and secondary coating with pitch. Three samples with different pitch contents of 30%, 40% and 50% were synthesized. The composition and morphology of the composites were characterized by X-ray diffractometry (XRD) and scanning electron microscopy (SEM), respectively, and the properties were tested by electrochemical measurements. The results indicated that the composites showed obviously enhanced electrochemical performance compared with that without secondary carbon coating. The second discharge capacity of the composite was 773 mA·h/g at a current density of 100 mA/g, and still retained 669 mA·h/g after 60 cycles with a small capacity fade of less than 0.23%/cycle, while the content of secondary carbon source of pitch was set at 40%. Therefore, the cycle stability of the composite could be excellently improved by regulating carbon content of secondary coating.

Key words: Si/C composite; secondary coating; coral structure; anode material; Li-ion battery

1 Introduction

Silicon, for its ultra-high theoretical Li-storage capacity (~3579 mA·h/g) [1], has attracted considerable attention as a promising anode candidate for the next generation Li-ion batteries (LIBs). Nevertheless, the large volume change (up to 300%) during lithiation and de-lithiation process easily causes mechanical cracks and further results in electrode pulverization. This leads to poor cycle performance of Si-based anodes, which greatly holds back its practical application. Many efforts have been concentrated on improving the cycle stability of Si-based anodes [2–5]. Constructing specific nanostructures, such as nanoparticles [6], nanowires [7], nanotubes [8] and nanofibers [9], is a significant strategy which can largely enhance the cycle performance. Besides, combining with stable matrix such as

graphene [10,11], C [12–14] and TiO₂ [15,16] is also often adopted.

A micro-sized Si/C composite consisting of interconnected Si and C nanoscale building blocks was once prepared as anode material and obtained a reversible capacity of 1459 mA·h/g after 200 cycles at 1 A/g with a capacity retention of 97.8% [13]. The influence of Si nanoscale building block size and C coating on the electrochemical performance of the micro-sized Si/C composites was further investigated, and subsequently a much better result was gained with a capacity of 1200 mA·h/g after 600 cycles at 1.2 A/g [1]. Another hard carbon@nanocrystalline Si@amorphous Si anode showed excellent capacity retention of 97.8% even after 200 cycles at 1C discharge/charge rate [14]. Besides, a hollow core-shell structured porous Si/C nanocomposite achieved a cycle capacity of ~760 mA·h/g after 100 cycles at 1 A/g [17]. Also, a capacity of

Foundation item: Project (11204090) supported by the National Natural Science Foundation of China; Project (2013KJCX0050) supported by the Department of Education of Guangdong Province, China; Projects (2014B040404067, 2014A040401005, 2015A040404043, 2015A090905003, 201508030033) supported by the Scientific and Technological Plan of Guangdong Province and Guangzhou City, China

Corresponding author: Ling-zhi ZHAO; Tel: +86-20-85215603; E-mail: lzzhao@vip.163.com
DOI: 10.1016/S1003-6326(15)64054-7

1053 mA·h/g after 100 cycles at 50 mA/g was manifested by a mesoporous Si@C microsphere anode [18]. Various carbon nanostructures were used to modify the silicon, and obviously enhanced electrochemical performance was achieved. Again, the influence of some factors was evaluated. Among these, the promoting role of carbon is evident. However, all the researches seem to be concentrated on zero-dimensional (0D), one-dimensional (1D) or two-dimensional (2D) nanocarbons only, the study on the three-dimensional (3D) carbon needs to be stressed. Moreover, the influence of secondary carbon coating on the properties of composites has not been systematically explored, and the necessity of secondary carbon coating has not been proved.

Herein, we reported a fabrication of the porous coral-structured Si/C composite by the method of coating PVA and secondary coating of pitch. The composition, surface morphology and electrochemical performance of the Si/C composite were characterized by X-ray diffractometry (XRD), scanning electron microscopy (SEM) and galvanostatic charge/discharge (GC) and cyclic voltammogram (CV) measurements. And the effect of the pitch content on the electrochemical performance of the Si/C composite anode was studied.

2 Experimental

2.1 Preparation

Figure 1 presents the synthesis scheme of the coral-structured Si/C composite.

In a typical synthesis procedure of hollow coral-structured Si/C composite, a certain amount of Si nanoparticles (<100 nm) were firstly dispersed in a mixture of 60 mL isopropyl alcohol (IPA) and 30 mL deionized water to form a uniform suspension, followed by the addition of 1.0 mL ammonia water. Then, 60 mL tetraethyl orthosilicate (TEOS)/IPA solution was added dropwise into the above suspension under vigorous stirring. The resulting suspension was continuously stirred for 12 h and then filtrated with a hybrid cellulose (0.22 μm) to obtain SiO₂-coated Si nanoparticles

(Si@SiO₂). The Si@SiO₂ was again dispersed in PVA solution (15 mg/mL) by 1 h ultrasonication. Mixing with 300 mL ethanol, the resulting floc was filtrated and dried in vacuum at 80 °C for 12 h. The dried floc was then calcined at 700 °C for 3 h with a heating rate of 3 °C/min under N₂ atmosphere. The gained powder was treated with 10% HF (mass fraction) solution to completely remove SiO₂ to get the Si@C composite. Next, it was coated with pitch by dispersing and solvent-evaporating with 30% pitch/tetrahydrofuran solution, and then calcined at 700 °C for 3 h under N₂ atmosphere to gain final porous coral-structured Si/C composites (Si@C@C-30%). As a comparison, Si@C@C-40% and Si@C@C-50% were synthesized with isometric 40% and 50% pitch/tetrahydrofuran solutions based on equivalent Si@C, respectively.

2.2 Electrodes and cells fabrication

Coin-type half cells were fabricated to evaluate the electrochemical properties. The anode slurry, which consisted of as-prepared products, conductive carbon blacks (Super P) and poly(vinylidene fluoride) (PVDF) at a mass ratio of 8:1:1, was uniformly coated on Cu foils and then cut into discs as electrodes after drying. N-methyl-2-pyrrolidone (NMP) was selected as slurry solvent. 1 mol/L LiPF₆ in a solvent mixture of ethylene carbonate and diethylene carbonate (1:1, volume fraction) and metal lithium were used as the electrolyte and the counter electrode, respectively.

2.3 Characterization

The composition, morphology and structure of the prepared samples were characterized by field-emission scanning electron microscopy (FESEM, ZEISS Ultra 55, 5 kV, Pt-spraying treatment), powder X-ray diffraction (XRD, BRUKER D8 ADVANCE, Cu K α radiation, $\lambda=1.5406$ nm). The charge/discharge tests of the assembled cells were performed on the LAND cell test system (LAND CT 2001A) at room temperature. And the electrode capacity was calculated based on the mass of the as-prepared products containing in the anode. Cyclic voltammetry (CV) experiment was carried out with an electrochemical analyzer (CHI 660D).

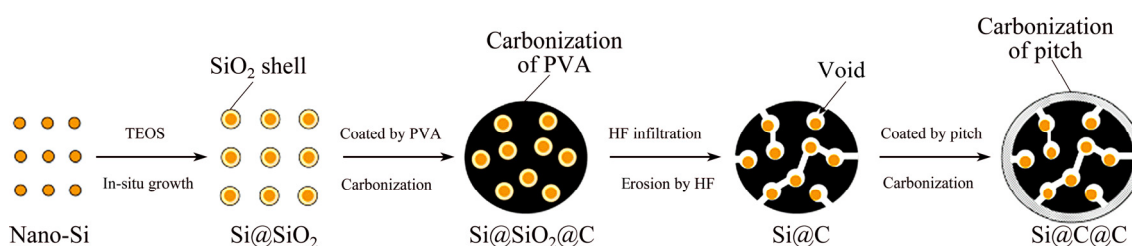


Fig. 1 Synthesis scheme of porous coral-structured Si/C (Si@C@C) composite

3 Results and discussion

3.1 Structure and morphology

Figure 2 shows the XRD patterns of pure Si and the as-prepared Si@C, Si@C@C-30%, Si@C@C-40% and Si@C@C-50%.

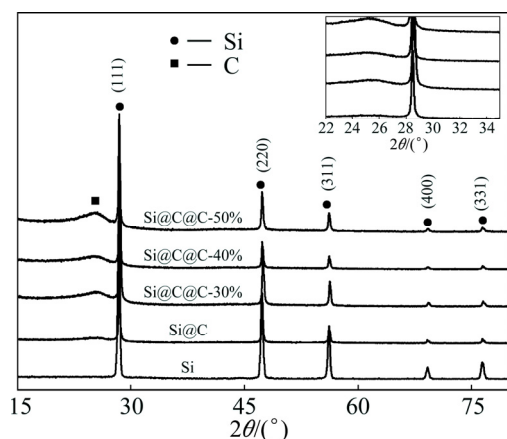


Fig. 2 XRD patterns of pure Si and as-prepared Si@C, Si@C@C-30%, Si@C@C-40% and Si@C@C-50%

All the sharp peaks can be indexed to crystal silicon (JCPDS No. 27–1402) and the blunt peaks are associated with carbon [19], indicating the successful synthesis of Si/C composites. Evidently, there is no other impurity peak in the patterns, and the position and shape of the silicon peaks have no significant change after coating with carbon, indicating that the pyrolysis does not destroy the original crystalline structure in the carbonization process [20]. By comparing the patterns of pure Si and Si@C, it can be seen that the blunt peak in the Si@C pattern can be easily ignored. This appears that all peaks around 25° refer to amorphous carbon. With the increase of pitch content, the relative intensity of the blunt peak in the composite pattern is gradually enhanced, since the effect shown in XRD patterns should be related only to the increase of carbon content.

Figure 3 presents SEM images of the as-prepared Si@SiO₂, Si@C, Si@C@C-30%, Si@C@C-40% and Si@C@C-50%. In Fig. 3(a), uniform nanoparticles can be clearly observed, indicating that the sphere shape is well maintained after coating with SiO₂. The average sizes of these particles are evaluated to be 100–200 nm. Then, Fig. 3(b) shows the image of Si@C after carbon coating and HF erosion. It can be seen that many pores are induced in the composites manifesting the successful removing of SiO₂. Furthermore, the carbon coatings are therefore converted to thin continuous micron carbon network, and there are many particles embedded in the hollow locations and partially exposed outside. The SEM images of the Si@C@C samples (Si@C@C-30%,

Si@C@C-40% and Si@C@C-50%) with secondary carbon coating are shown in Figs. 3(c)–(e). Noting that, in Fig. 3(c), there are still many hollow pores with silicon particles directly exposed outside with insufficient secondary carbon coating. Then, in Fig. 3(d), it can be seen that the Si@C structure is well coated by the second carbon coating. No obvious silicon particles are directly exposed outside, and many pores are preserved in the new Si@C@C composite to successfully form the porous coral structure. While in Fig. 3(e), though the silicon particles are fully coated by the secondary carbon coating, lots of pores are infilled with excessive secondary carbon which leads to large condensed block and is useless for the relief of negative effect caused by volume change.

3.2 Electrochemical performance

Figure 4 shows the cyclic voltammograms of the as-prepared Si@C, Si@C@C-30%, Si@C@C-40% and Si@C@C-50% composites at a scanning rate of 0.1 mV/s. It can be seen that the reduction currents at the potentials lower than 1.3 V from the negative sweep of the 1st cycle correspond to the lithium intercalation and mainly to the formation of solid electrolyte interphase (SEI) film, and the oxidation current peaks from 0.001 to 1.5 V correspond to the lithium de-intercalation. The peak at around 1.3 V can be observed in every sample in the 1st discharge. This would be attributed to the insertion of lithium ions into the disordered carbon phase, and then this peak disappears in subsequent cycles [21]. It should be noticed that the current peak for SEI layer formation still exists in the initial cycles, which accounts for the initial capacity loss of these anodes. These current peaks would be hardly observed gradually, indicating that the stable charge–discharge cycles begin on the anodes. In the 5th cycle, all the current peaks can be clearly observed. The main current peak for the Li–Si alloying appears at 0.25 V and the corresponding current peak of the dealloy of lithium ions from silicon can be observed when the potential is reversed, corresponding to lithiation and de-lithiation of amorphous Li–Si alloys [22], respectively. And the shape and position of them are similar for four samples, as shown in Fig. 4, except the great difference in the 1st cycle.

In Fig. 4(a), the significant current for the SEI layer formation at the potentials from 1.5 to 0.5 V can be observed in the 1st discharge, suggesting that the fresh Si surface is available during discharge process. This should be ascribed to the direct exposure of silicon surface to electrolyte after HF erosion, just as shown in Fig. 3(b). This large current in the 1st discharge accounts for the loss of the capacity. As comparison, the smaller currents appear at potentials from 1.3 to 0.5 V in the 1st cycle

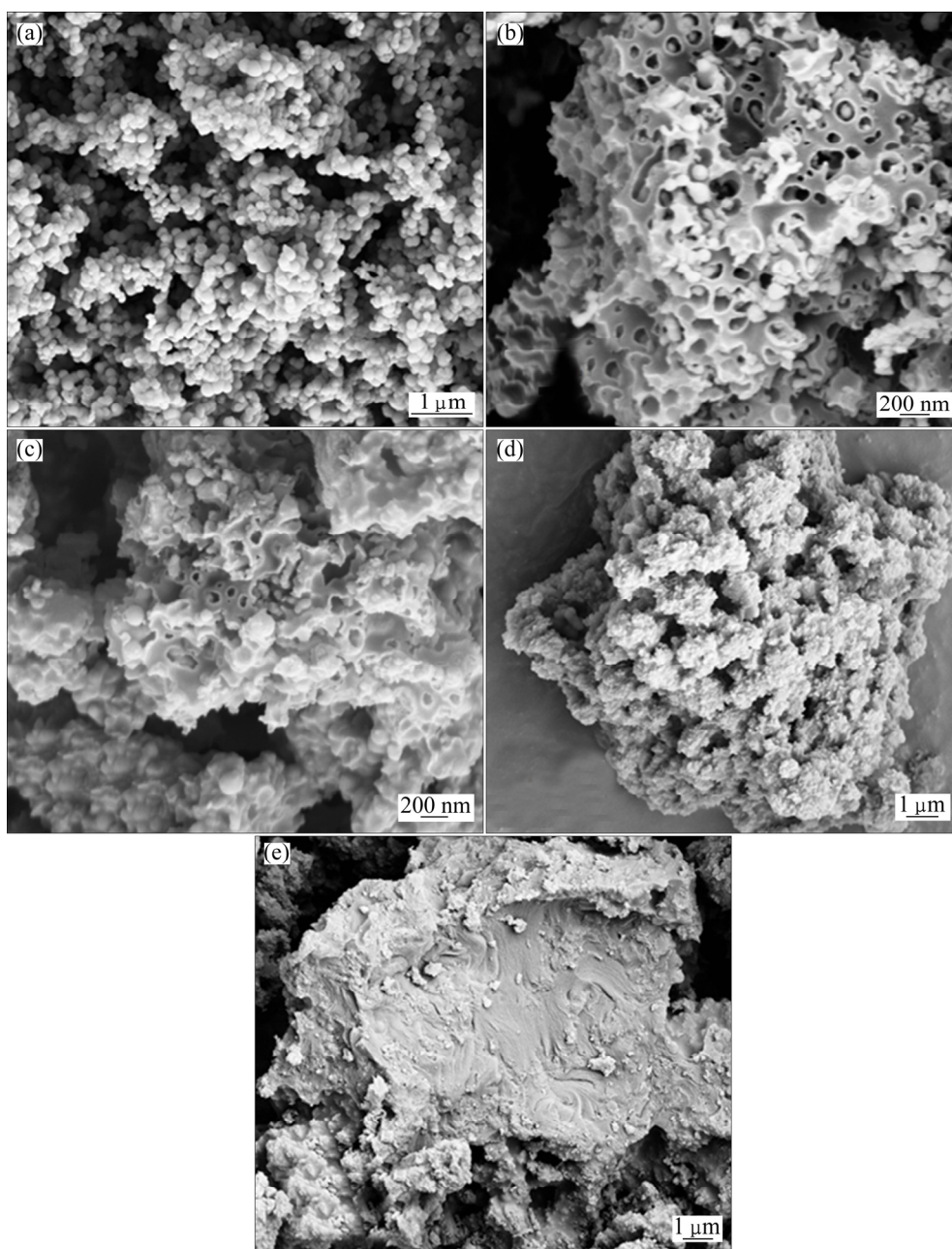


Fig. 3 SEM images of as-prepared Si@SiO₂ (a), Si@C (b), Si@C@C-30% (c), Si@C@C-40% (d) and Si@C@C-50% (e)

after the composites were coated by pyrolytic carbon from pitch, as shown in Figs. 4(b)–(d), which would lead to less loss of lithium insertion capacity of the anodes. With the increase of pitch content in the coating layer, at potentials lower than 0.5 V in the 1st discharge, the current becomes much larger. This can be ascribed to the SEI formation on carbon surface and the insertion of lithium ions into carbon taking place quickly when a lot of carbon is available, since the related reactions of carbon anode occur at a low potential.

Figure 5 shows the potential profiles of the as-prepared Si@C, Si@C@C-30%, Si@C@C-40% and Si@C@C-50% composites in the range of 0.01–1.0 V, when the current density is 100 mA/g. An obvious

plateau at 0–0.2 V can be observed for the 1st discharge processes of all samples, which accounts for the initial, irreversible transformation of crystalline Si to amorphous Li–Si [23].

The plateau of the composite without pitch appears at the potential of 1.5 V, as shown in Fig. 5(a), which is higher than that at about 1.25 V when the composites are coated by pyrolytic carbon from pitch, as shown in Figs. 5(b)–(d). This should be ascribed to the avoidance of direct exposure of silicon surface after coating with pitch. In the 5th cycle, the discharge plateau around 0.5 V can be also observed. These results are in accordance with the data from their cyclic voltammograms shown in Fig. 4.

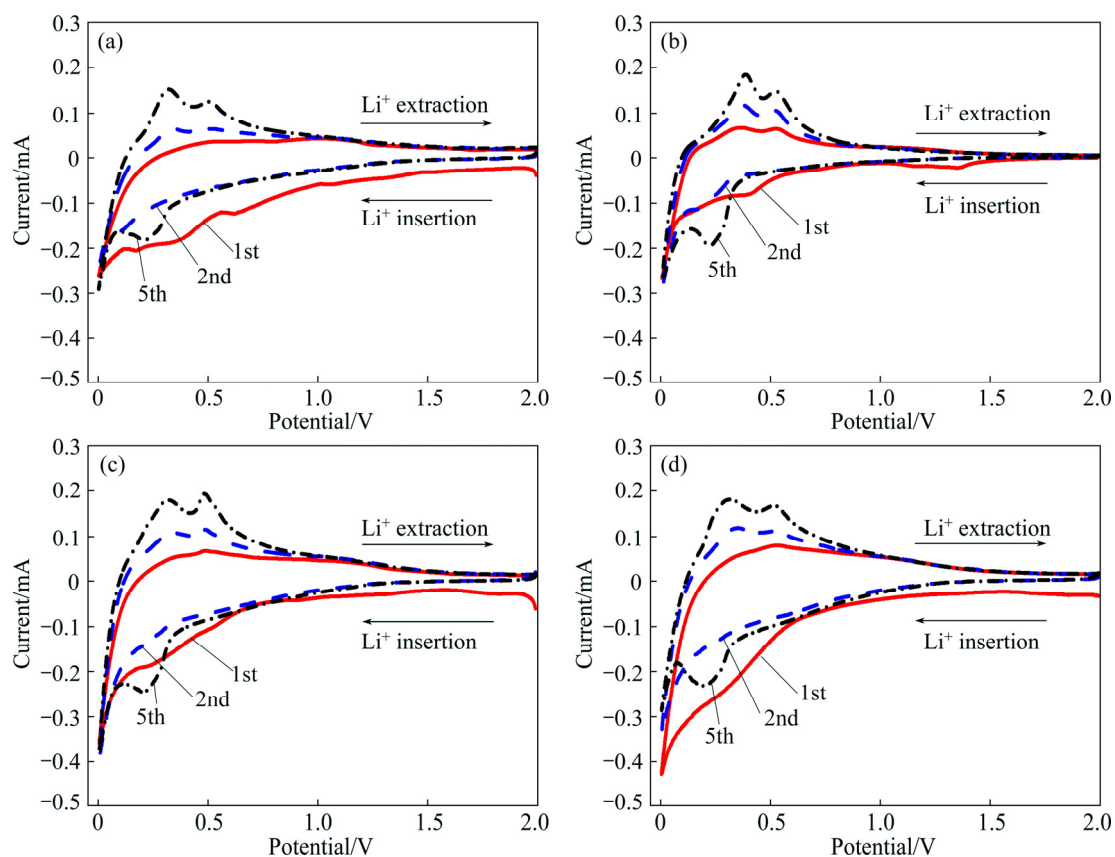


Fig. 4 Cyclic voltammograms of as-prepared Si@C (a), Si@C@C-30% (b), Si@C@C-40% (c) and Si@C@C-50% (d)

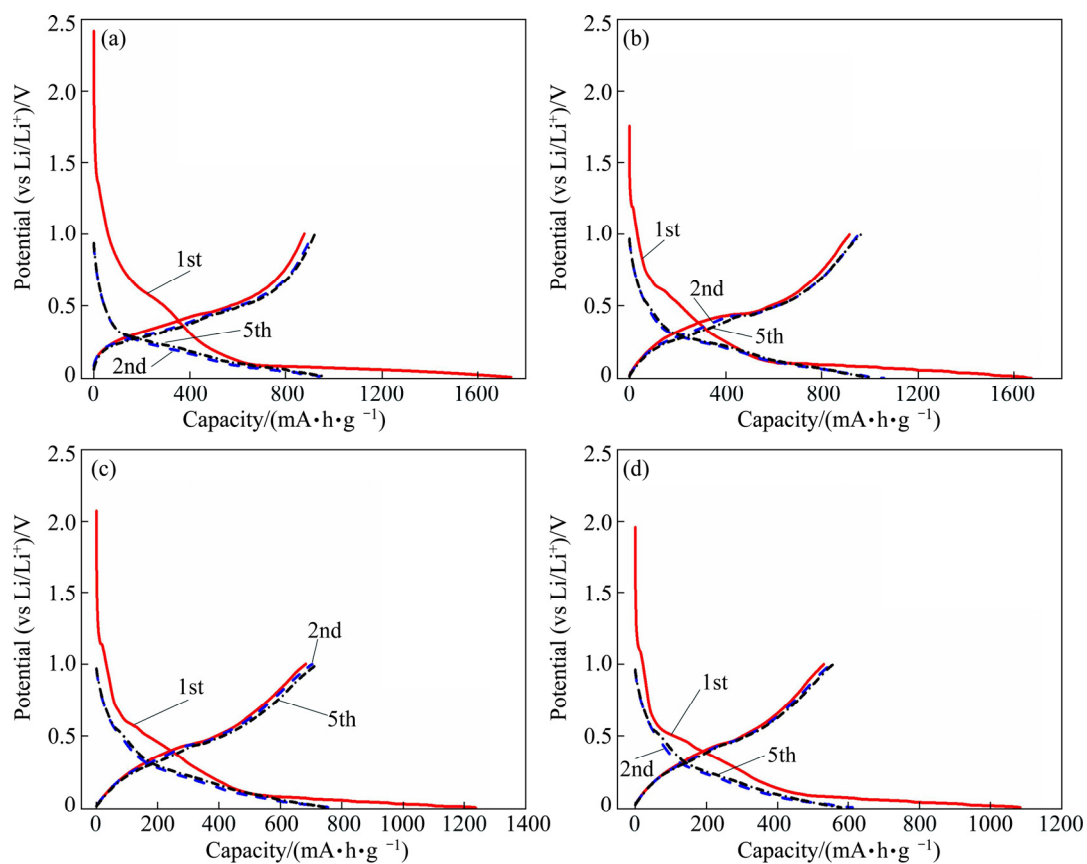


Fig. 5 Discharge and charge curves of as-prepared Si@C (a), Si@C@C-30% (b), Si@C@C-40% (c) and Si@C@C-50% (d)

The discharge and charge capacities, the initial capacity loss and the coulombic efficiency of these electrodes in the 1st cycle are listed in Table 1. It should be noticed from Table 1 that, as pitch content (mass fraction) increases from 0 to 50%, the discharge capacity is reduced gradually, which changes from 1739 to 1082 mA·h/g. This should be ascribed to the higher theoretical specific capacity of silicon than that of carbon. The initial capacity loss of the samples also decreases gradually from 862 to 470 mA·h/g, corresponding to the increase of the coulombic efficiency from 50.4% to 56.5%. This indicates that, after secondary coating of pitch in fabrication process, the formation of unnecessary SEI layer that would lead to large irreversible capacity loss is efficiently constrained. It is obvious that the method of secondary coating reduces the initial capacity but improves the coulombic efficiency and the reversible capacity.

Table 1 Charge/discharge parameters of coral structured hollow Si/C composites without and with 30%, 40% and 50% pitch in the 1st cycle

Mass fraction of pitch/%	Discharge capacity/(mA·h·g ⁻¹)	Charge capacity/(mA·h·g ⁻¹)	Initial capacity loss/(mA·h·g ⁻¹)	Coulombic efficiency/%
0	1739	877	862	50.4
30	1673	917	756	54.8
40	1237	683	554	55.2
50	1082	612	470	56.5

Figure 6 shows the electrochemical performance of as-prepared materials. Major performance values obtained from Fig. 6(a) are listed in Table 2. It can be found that the discharge capacity of Si@C decreases quickly with increasing cycle number. When the pitch content is higher than 40%, the coulombic efficiency becomes close to 100% after the 7th cycle. Obviously, the cyclic performance of the hollow Si/C composites is significantly improved after secondary coating of pitch. This suggests that the method of secondary coating can strengthen the cyclic stability for lithium intercalation and de-intercalation of the anodes and therefore maintain higher reversible capacity and coulombic efficiency.

As can be seen from Table 2, the Si/C composite with 40% pitch exhibits the least capacity loss and the best capacity retention among all the samples, keeping 86.55% of the 2nd discharge capacity after the 60th cycle. This demonstrates that the appropriate ratio of the pitch used for secondary coating Si/C composite would be good to not only provide the integrated and stable core-shell structure of the composite, but also hold the high capacity in deep cycles. After 60 cycles, its

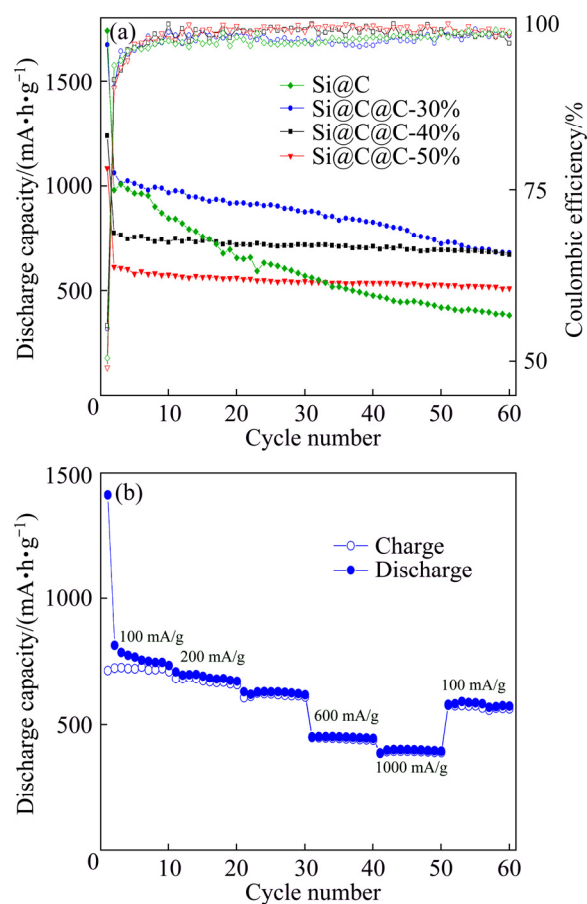


Fig. 6 Cyclic performance of Si@C, Si@C@C-30%, Si@C@C-40% and Si@C@C-50% (a), and rate capability of hollow Si/C composite with 40% pitch at current densities of 100, 200, 400, 600 and 1000 mA/g (b)

discharge capacity is 669 mA·h/g, and there is only a small capacity fade of less than 0.23%/cycle from the 2nd to 60th cycle. This improvement can be ascribed to the accommodation of silicon volume expansion during lithiation and de-lithiation process by the sufficient void space from inner carbon structure, just as shown in Fig. 3(b), and the structural stability of the composite by the secondary coating layer from pitch, just as shown in Figs. 3(c)–(e). Then, the integrity of electrode and good electrical contact between silicon and conducting agents are maintained.

Figure 6(b) shows the rate capability of the hollow Si/C composite with 40% pitch at current densities of 100, 200, 400, 600 and 1000 mA/g. The cell is cycled at a current density of 100 mA/g for the initial 10 cycles. Then, the current density is gradually increased to 200, 400, 600 and 1000 mA/g for every 10 cycles and finally returns to 100 mA/g for the last 10 cycles. It is found that there is a discharge capacity of 1411 mA·h/g at a current density of 100 mA/g in the 1st cycle. After 10 cycles, the cell displays an average reversible capacity of about 688 mA·h/g at a current density of 200 mA/g. As the

Table 2 Cyclic performance parameters of coral structured hollow Si/C composites without and with 30%, 40% and 50% pitch after 60 cycles

Mass fraction of pitch/%	Discharge capacity in 1st cycle/ (mA·h·g ⁻¹)	Discharge capacity in 2nd cycle/ (mA·h·g ⁻¹)	Discharge capacity in 60th cycle/ (mA·h·g ⁻¹)	Capacity loss from 1st to 2nd cycle/ (mA·h·g ⁻¹)	Capacity retention from 2nd to 60th cycle/%
0	1739	979	383	760	39.12
30	1673	1061	678	612	63.90
40	1237	773	669	464	86.55
50	1082	612	510	470	83.33

current densities increase to 400, 600 and 1000 mA/g, the average reversible capacities become 624, 450 and 398 mA·h/g, respectively. When the current density is directly reduced back to 100 mA·h/g, the reversible capacity quickly increases to 578 mA·h/g, indicating that the coral structured hollow Si/C composite with pitch exhibits an excellent rate capability. It should be ascribed to the stable 3D network inner structure, just as shown in Fig. 3(b), which would act as a vital pathway for rapid ion/electron diffusion or transmission.

4 Conclusions

1) The coral structured hollow Si/C composite can be synthesized by a simple and low-cost approach.

2) The electrochemical performance of the Si/C composite can be greatly improved by secondary coating of pitch.

3) The prepared composites manifest excellent electrochemical performance, especially at the secondary carbon source usage of 40%, with a capacity of 669 mA·h/g after 60 cycles. The synergetic effect of the initial and secondary carbon coating, as well as the coral structure, should be responsible for the enhanced performance.

References

- [1] YI R, DAI F, GORDIN M L, SOHN H, WANG D. Influence of silicon nanoscale building blocks size and carbon coating on the performance of micro-sized Si-C composite Li-ion anodes [J]. *Advanced Energy Materials*, 2013, 3(11): 1507–1515.
- [2] YUAN Q, ZHAO F, ZHAO Y, LIANG Z, YAN D. Evaluation and performance improvement of Si/SiO₂/C based composite as anode material for lithium ion batteries [J]. *Electrochimica Acta*, 2014, 115(3): 16–21.
- [3] SI Q, HANAI K, ICHIKAWA T, HIRANO A, IMANISHI N, YAMAMOTO O, TAKEDA Y. Improvement of cyclic behavior of a ball-milled SiO and carbon nanofiber composite anode for lithium-ion batteries [J]. *J Power Sources*, 2011, 196(22): 9774–9779.
- [4] WANG B, LI X, ZHANG X, LUO B, JIN M, LIANG M, DAYEH S A, PICRAUX S T, ZHI L. Adaptable silicon-carbon nanocables sandwiched between reduced graphene oxide sheets as lithium ion battery anodes [J]. *ACS Nano*, 2013, 7(2): 1437–1445.
- [5] FU K, XUE L, YILDIZ O, LI S, LEE H, LI Y, XU G, ZHOU L, BRADFORD P D, ZHANG X. Effect of CVD carbon coatings on Si@CNF composite as anode for lithium-ion batteries [J]. *Nano Energy*, 2013, 2(5): 976–986.
- [6] LIU X, ZHONG L, HUANG S, MAO S, ZHU T, HUANG J. Size-dependent fracture of silicon nanoparticles during lithiation [J]. *ACS Nano*, 2012, 6(2): 1522–1531.
- [7] CHAN C K, PATEL R N, O'CONNELL M J, KORGEL B A, CUI Y. Solution-grown silicon nanowires for lithium-ion battery anodes [J]. *ACS Nano*, 2010, 4(3): 1443–1450.
- [8] SONG T, XIA J, LEE J H, LEE D H, KWON M S, CHOI J M, WU J, DOO S K, CHANG H, PARK W, ZANG D S, KIM H, HUANG Y. Arrays of sealed silicon nanotubes as anodes for lithium ion batteries [J]. *Nano Letters*, 2010, 10(5): 1710–1716.
- [9] TANG Jing-jing, YANG Juan, ZHOU Xiang-yang, CHEN Guang-hui, HUANG Bin. Synthesis of one-dimensional carbon nanostructures and their application as anode materials in lithium ion batteries [J]. *Transactions of Nonferrous Metals Society of China*, 2014, 24(4): 1079–1085.
- [10] EOM K S, JOSHI T, BORDES A, DO I, FULLER T F. The design of a Li-ion full cell battery using a nano silicon and nano multi-layer graphene composite anode [J]. *J Power Sources*, 2014, 249(3): 118–124.
- [11] LAI Jun, GUO Hua-jun, LI Xiang-qun, WANG Zhi-xing, LI Xin-hai, ZHANG Xiao-ping, HUANG Si-lin, GAN Lei. Silicon/flake graphite/carbon anode materials prepared with different dispersants by spray-drying method for lithium ion batteries [J]. *Transactions of Nonferrous Metals Society of China*, 2013, 23(5): 1413–1420.
- [12] TERRANOVAM L, ORLANDUCCI S, TAMBURRI E, GUGLIEMOTTI V, ROSSI M. Si/C hybrid nanostructures for Li-ion anodes: An overview [J]. *J Power Sources*, 2014, 246(3): 167–177.
- [13] YI R, DAI F, GORDIN M L, CHEN S, WANG D. Micro-sized Si-C composite with interconnected nanoscale building blocks as high-performance anodes for practical application in lithium-ion batteries [J]. *Adv Energy Mater*, 2013, 3(3): 295–300.
- [14] KIM C, KO M, YOO S, CHAE S, CHOI S, LEE E H, KO S, LEE S Y, CHO J, PARK S. Novel design of ultra-fast Si anodes for Li-ion batteries: Crystalline Si@amorphous Si encapsulating hard carbon [J]. *Nanoscale*, 2014, 6(18): 10604–10610.
- [15] YAN D, BAI Y, YU C, LI X, ZHANG W. A novel pineapple-structured Si/TiO₂ composite as anode material for lithium ion batteries [J]. *Journal of Alloys and Compounds*, 2014, 609(26): 86–92.
- [16] LOTFABAD E M, KALISVAART P, KOHANDEHQHAN A, CUI K, KUPSTA M, FARBOD B, MITLIN D. Si nanotubes ALD coated with TiO₂, TiN or Al₂O₃ as high performance lithium ion battery anodes [J]. *J Mater Chem A*, 2014, 2(8): 2504–2516.
- [17] LI X, MEDURI P, CHEN X, QI W, ENGELHARD M H, XU W, DING F, XIAO J, WANG W, WANG C, ZHANG J, LIU J. Hollow core-shell structured porous Si-C nanocomposites for Li-ion battery anodes [J]. *J Mater Chem*, 2012, 22(22): 11014–11017.
- [18] MA X, LIU M, GAN L, TRIPATHI P K, ZHAO Y, ZHU D, XU Z, CHEN L. Novel mesoporous Si@C microspheres as anodes for

- lithium-ion batteries [J]. *Phys Chem Chem Phys*, 2014, 16(9): 4135–4142.
- [19] XIAO J, XU W, WANG D, CHOI D, WANG W, LI X, GRAFF G L, LIU J, ZHANG J. Stabilization of silicon anode for li-ion batteries[J]. *Journal of the Electrochemical Society*, 2010, 157(10): A1047–A1051.
- [20] WANG M S, FAN L Z. Silicon/carbon nanocomposite pyrolyzed from phenolic resin as anode materials for lithium-ion batteries [J]. *J Power Sources*, 2013, 244(4): 570–574.
- [21] WANG L, DING C X, ZHANG L C, XU H W, ZHANG D W, CHENG T, CHEN C H. A novel carbon–silicon composite nanofiber prepared via electrospinning as anode material for high energy-density lithium ion batteries [J]. *J Power Sources*, 2010, 195(15): 5052–5056.
- [22] HUANG X, PU H, CHANG J, CUI S, HALLAC P B, JIANG J, HURLEY P T, CHEN J. Improved cyclic performance of Si anodes for lithium-ion batteries by forming intermetallic interphases between Si nanoparticles and metal microparticles [J]. *ACS Appl Mater Interfaces*, 2013, 5(22): 11965–11970.
- [23] OBROVAC M N, CHRISTENSEN L. Structural changes in silicon anodes during lithium insertion/extraction [J]. *Electrochem Solid-State Lett*, 2004, 7(5): A93–A96.

用于锂离子电池的多孔珊瑚状硅/碳复合负极材料的合成、表征及电化学性能

唐芬玲^{1,2}, 雷建飞³, 崔朝阳¹, 欧阳剑¹, 刘钢¹, 赵灵智^{1,4}

1. 华南师范大学 光电子材料与技术研究所 广东省微纳光子功能材料与器件重点实验室, 广州 510631;
2. 广东省食品药品职业技术学校, 广州 510663;
3. 河南科技大学 物理和工程学院, 洛阳 471023;
4. 广东省低碳与新能源材料工程技术研究中心, 广州 510631

摘要: 利用 PVA 碳源包覆、HF 酸刻蚀和沥青二次包覆方法制备多孔珊瑚状硅/碳复合负极材料, 得到沥青含量分别为 30%、40%和 50%(质量分数)的 3 种硅/碳复合材料样品。采用 XRD 和 SEM 分别对复合材料的组成和形貌进行表征, 并采用电化学测试手段对其性能进行测试。结果表明, 经二次沥青包覆后, 复合材料的电化学性能得到明显提高。当二次包覆的沥青含量为 40%时, 在 100 mA/g 的电流密度下, 该样品第二次充放电循环的放电容量达到 773 mA·h/g, 经 60 次循环后, 放电容量仍然保持在 669 mA·h/g, 其容量损失率仅为 0.23%/cycle。因此, 调整二次包覆碳含量可明显改善复合材料的循环稳定性。

关键词: 硅/碳复合材料; 二次包覆; 珊瑚状结构; 负极材料; 锂离子电池

(Edited by Wei-ping CHEN)